THE ASTRONOMICAL JOURNAL VOLUME 110, NUMBER 4 OCTOBER 1995

QUASAR RADIO MORPHOLOGY AND CLUSTERING ENVIRONMENT AT $z\sim1/2$

TRAVIS A. RECTOR, JOHN T. STOCKE, AND ERICA ELLINGSON

Center for Astrophysics and Space Astronomy, University of Colorado, Boulder, Colorado 80309-0389
Electronic mail: rector@casa.colorado.edu, stocke@hyades.colorado.edu, ellingso@pisco.colorado.edu

Received 1995 February 9; revised 1995 June 9

ABSTRACT

The radio morphology of 30 radio-loud quasars at $z\sim\frac{1}{2}$ is studied as a function of cluster density using data available in the literature. While correlations between several morphological parameters of the radio emission are consistent with interactions with an intracluster medium (ICM), we do not see the correlation between galaxy density and quasar radio morphology expected from ICM interaction. Therefore, distorted radio morphology is not an indicator for the presence of a distant cluster as previously suggested. Because such correlations are found at $z\sim0$, these results are suggestive that the rich clusters containing quasars at $z\sim\frac{1}{2}$ have not yet developed a dense ICM. An inelastic collision with neighboring galaxies and intergalactic clouds can account for the morphology of several of the sources in this sample and is a viable alternative explanation. © *1995 American Astronomical Society.*

1. INTRODUCTION

Powerful ($P>10^{25}$ W Hz^{-1}) edge-brightened double radio sources, also referred to as "classic doubles," "symmetric doubles," "Cygnus A-type doubles," "Fanaroff–Riley type II doubles (FR-II)," and also "triples," have several morphological characteristics in common. Most are nearly symmetric (i.e., the lobes are comparable in size and luminosity), collinear (i.e., the central core and both outer lobes lie upon the same line), with hotspots close to the extremities of the lobes and weak, one sided jets. "Fanaroff–Riley type I doubles (FR-I)," are edge dimmed, asymmetric, and distorted (i.e., not collinear as defined above). FR-I sources are also less luminous than FR-IIs and typically have two-sided jets. Typical cluster radio galaxies such as "wide-angle-tails" (WATs) and narrow-angle-tails (NATs) are types of FR-I morphologies. Previous studies (De Young 1976; Stocke 1979; Longair & Seldner 1979) have confirmed that the relative sizes and distortions of FR-I sources compared to FR-II sources support the picture that the dense ICM in clusters of galaxies causes the distorted radio morphologies observed at $z\sim0$. This dense ICM is now directly detected due to its luminous x-ray emission (e.g., Forman & Jones 1982). The distortions in type I objects are often attributed to the motion of the source relative to a dense ICM (Jaffe & Perola 1973; Jones & Owen 1979). Quasars, which are usually classified as FR-II due to their luminosity and morphology, occasionally show distortion in their structure similar to type I sources; but it is unclear whether or not these distortions are caused by interaction with an ICM. A correlation between the morphology of a quasar and its environment (i.e., is it in a cluster?) would provide strong evidence that a dense ICM is present and is responsible for distorted radio morphologies at $z\sim\frac{1}{2}$, where direct detection of x-ray emission is not currently possible.

Expecting this effect to be present, Hintzen & Scott (1978) proposed that distant quasars with noncollinear structure are members of clusters and that distorted quasar radio sources may be tracers for clusters too distant to detect easily. However, Stocke *et al.* (1985) presented observations of four quasars which suggest the contrary. They argued that the morphologies of distant quasars do not resemble cluster FR-I sources but instead their bent, or "dogleg" FR-II morphology can be accounted for by the collision between the outwardly moving radio jet and a single gas cloud, most likely associated with a single cluster galaxy.

In this paper we attempt to detect a correlation between the quasar-galaxy spatial covariance amplitude B_{gq} (i.e., cluster galaxy density around the quasar) as previously measured by Yee & Ellingson (1993) and four radio morphological characteristics: hotspot location, projected bending angle, physical size and length asymmetry for a sample of quasars at $0.26<z<0.62$. If present, such correlations would provide strong evidence to support ICM interactions as the dominant cause of distortion in the extended radio emission of distant quasars and would indirectly suggest that distant rich clusters which have quasars near their centers possess a dense ICM. We also look for correlation between the core and total radio power and radio morphology that, if strong, would suggest that radio power, not a dense ICM, is the dominant factor in determining a quasar's radio morphology (e.g., Owen & Ledlow 1994). We also look for correlation between the morphological characteristics to test for consistency within the sample.

2. THE SAMPLE

Fifty-four radio-loud quasars RLQs with 3C, 4C, 5C, or PKS identifications were initially chosen from the optical imaging study of Yee & Ellingson (1993, hereafter referred to as YE93) for which the cluster density B_{gq} and redshift z were given. For 40 of these sources we were able to determine the largest angular size (LAS), hence the physical size, from the literature (primarily from Hintzen *et al.* 1983). We were also able to obtain radio maps for 38 of these sources. Of these, 31 were "triple" (sources consisting of a central core and two outer lobes are hereafter called "triple" sources even though they are commonly called "classic doubles,"

 0004-6256/95/110(4)/1492/6/$0.90

TABLE 1. Radio morphological properties and environment of the sample.

Name	Alt Name	z	B_{gq}	±	Ref	*LAS*	Size	θ	*FR*	Q
0003+158	4C 15.01	0.450	473	174	S	31.0	210.8	0	> 0.73	1.2
0135−057	4C -05.06	0.400	-47	139	H	40.5	226.2	65	0.88	1.2
0137+012	4C 01.04	0.260	313	176	H	27.0	136.0	1	0.77	1.9
0155−109	PKS	0.616	777	273	S	3.2*	24.6	25	> 0.59	1.3
0349−146	3C 95	0.614	737	337	P	114.0	874.3	3	0.92	1.1
0405−123	PKS	0.574	905	277	M	19.0	142.4	11	0.88	1.4
0742+318	4C 31.30	0.462	145	181	N	115.0	791.1	4	0.83	1.1
0805+578	4C 57.15	0.438	512	262	H	26.0	174.6	1	0.79	1.1
0846+100	4C 09.31	0.366	111	149	G	54.0	331.9	16	0.91	1.5
0903+169	3CR 215	0.411	1000	242	P	43.0	280.2	58*	0.77	1.2
1012+488	4C 48.28	0.385	120	181	H	109.0	687.7	8	0.91	1.1
1058+110	4C 10.30	0.423	160	131	MH	31.0	204.8	4	0.71	1.0
1100+772	3CR 249.1	0.311	-38	141	PH	21.0	117.9	9	> 0.72	1.7
1103−006	4C -0.43	0.422	-46	98	S	21.0	138.6	3	0.86	1.5
1104+167	4C 16.30	0.634	943	381	H	40.0	309.9	5	0.92	1.0
1146−037	PKS	0.341	91	141	S	193.0	1142.0	12	0.94	1.1
1156+631	4C 63.15	0.594	653	388	P	58.0	440.0	5	0.94	1.4
1200−051	PKS	0.381	320	208	S	6.9*	43.3	27	0.81	1.0
1217+023	PKS	0.240	299	167	N	110.0	526.0	0	0.70	1.0
1241+166	3CR 275.1	0.557	1125	399	S	14.0	103.8	22	0.84	1.5
1302−102	PKS	0.286	210	178	G	17.4*	93.0	60*	> 0.79	1.0
1352−104	PKS	0.332	107	145	S	36.0*	209.9	28	0.76	2.2
1512+370	4C 37.43	0.370	42	218	PW	61.0	377.1	0	> 0.71	1.2
1545+210	3CR 323.1	0.264	440	224	G	70.5	358.5	4	0.91	1.4
1548+114	4C 11.50A	0.436	304	157	H	50.0	335.1	47*	0.84	1.1
1618+177	3CR 334	0.555	187	220	S	46.0	340.7	3	0.91	1.6
1704+608	3CR 351	0.370	-198	138	P	58.0	358.5	12	0.90	1.2
2209+080	4C 08.64	0.484	273	210	H	10.5	73.7	17	> 0.81	1.9
2251+113	4C 11.72	0.323	315	286	P	9.8	56.3	1	0.81	1.6
2314−116	PKS	0.549	-29	154	P	47.5*	350.4	14	0.88	1.7

TABLE 2. Radio powers of the sample.

Name	S_6^c	S_{20}^c	α_{core}	Ref	S_6^t	S_{20}^t	Ref	$logP_{20}^c$	$logP_{20}^t$
0003+158	125	···	0.28	Hu	···	590	PKS	24.72	25.54
0135−057	···	123	···	H	···	201	H	24.81	25.03
0137+012	150	230	-0.35	G	···	1125	H	24.87	25.56
0155−109	···	···	···	···	···	2000	PKS	···	26.17
0349−146	45	···	0.21	Hu	···	2800	PKS	24.42	26.32
0405−123	···	···	···	···	···	3200	PKS	···	26.36
0742+318	640	610	0.04	G	843	···	B	25.56	25.34
0805+578	26	···	0.31	Hu	···	969	Hu	24.01	25.75
0846+100	6	7	-0.13	G	···	600	PKS	23.53	25.46
0903+169	18	···	0.59	Hu	···	962	H	23.69	25.72
1012+488	···	36	···	Hu	···	150	H	24.26	24.88
1058+110	···	···	···	···	···	916*	PKS	···	25.71
1100+772	100	···	-0.80	K,C	775	···	HR	25.03	25.92
1103−006	76	···	···	K	···	1061	H	24.89	25.77
1104+167	388	···	0.32	Hu	···	695	H	25.31	25.73
1146−037	···	115	···	Hu	···	314	H	24.71	25.15
1156+631	13	···	0.22	Hu	···	997	Hu	24.72	26.40
1200−051	···	···	···	···	···	546*	PKS	···	25.44
1217+023	320	220	0.24	G	···	610	PKS	24.81	25.25
1241+166	130	···	-0.80	K,C	···	2900	PKS	25.38	26.31
1302−102	780	···	0.61	K	···	786	PKS	25.32	25.46
1352−104	···	···	···	···	···	628*	PKS	···	25.43
1512+370	62	···	···	K	···	385	H	24.74	25.65
1545+210	32	···	-0.70	K,C	···	2011	H	24.39	25.90
1548+114	414	···	0.84	Hu	···	592*	PKS	24.94	25.34
1618+177	133	···	-0.19	Hu	···	2200	PKS	25.07	26.15
1704+608	8	···	-0.93	Hu	1230	···	K	24.09	26.17
2209+080	225	···	-0.40	Hu	···	1731	H	25.36	26.04
2251+113	18	···	-0.70	Hu	···	1438	H	24.25	25.78
2314−116	91	···	0.10	Hu	···	1630	PKS	24.75	25.28

etc.). Sources with one outer lobe or no lobes were discarded because the presence of a second lobe is unknown; hence, any measure of physical size is suspect and no bending angle can be measured. One source (PKS 2349−014) is at a substantially lower redshift (z=0.18) than the others and has been eliminated for that reason. Given that the sources deleted here were not heavily dominated by low or high B_{gq} values, we expect no bias with respect to the full sample of 54 quasars. YE93 present evidence that their sample is not biased with respect to known factors. Our final source list consists of these 30 "triple" sources for which we were able to obtain or measure reliably the following quantities: cluster density B_{gq}(YE93), the redshift z, the physical size, the projected bending angle θ, and the length asymmetry; these data are shown in Table 1. We were able to determine the core radio power at 20 cm for only 24 of these sources; their radio powers at 20 cm are listed in Table 2. The contents of these tables are described in detail in the next section.

3. QUANTITATIVE MEASUREMENTS OF RADIO MORPHOLOGY, RADIO POWER, AND ENVIRONMENT

For the sources for which we were able to obtain a radio map, we measured the bending angle θ between the central core and the outer lobes, the largest angular size Ψ, and the Fanaroff–Riley (FR) ratio (see Fig. 1 and below for definitions). The bending angle is defined as the angle of intersection between the two lines connecting the flux peaks of each outer lobe with the central component (Hintzen *et al.* 1983).

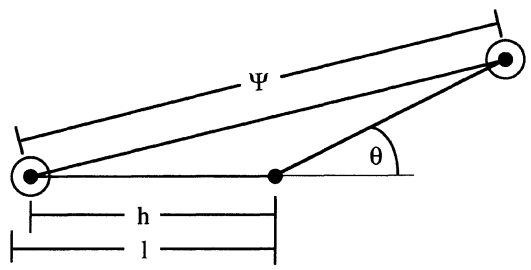

FIG. 1. The geometry for measuring the bending angle θ, the largest angular size Ψ, the length asymmetry Q, and the FR ratio for a source.

The bending angle is a measure of noncollinearity; the bending angle $\theta=0°$ if the source is perfectly collinear. θ was measured to within $\sim 1°$. For some objects the bending angle is not clear (e.g., due to multiple "knots" in the lobe); for these sources a plausible range of bending angle is listed in the comments on individual sources. The peak flux, or "hot spot," is interpreted in beam models as the location at which the jet carrying the energy encounters the lobe. Thus the measure of θ is more a measure of asymmetries in the beam rather than the structure of the outer lobes (Hintzen *et al.* 1983). The largest angular size Ψ is measured between the bright spots in the outer lobes, not the outer edges so that the measured size is not dependent on instrumental sensitivity.

We calculated the physical size of the source using the largest angular size Ψ, redshift z, and standard Friedmann–Robertson–Walker cosmological model assuming a Hubble constant $H_0=100$ km s^{-1} Mpc^{-1} and deceleration parameter $q_0=\frac{1}{2}$. The length asymmetry Q is defined as $Q=h_1/h_2$; h_1 and h_2 are defined (Fig. 1) as the distances between the central core and the regions of highest brightness in the outer lobes, i.e., the hotspots (McCarthy *et al.* 1991).

The FR ratio is defined by the equation:

$$\mathrm{FR}=\frac{h_1+h_2}{l_1+l_2},$$

where h_1 and h_2 are defined as above; and l_1 and l_2 are the distances between the core and the furthest extent of the outer lobes measured out to the 1% contour (Fig 1.). FR-II sources have FR$\approx$1 while FR-I sources have FR$\leqslant\frac{1}{2}$. Only one source in this sample, PKS 0155−109, has all three indicators of FR-I morphology: small physical size, large bending angle, and FR$\approx\frac{1}{2}$. This quasar also appear to be in a moderately rich cluster of galaxies given its $B_{\mathrm{gq}}\approx 777$ Mpc$^{-1.8}$. However, the available map has insufficient resolution to accurately determine the FR ratio. Given the small size of this source an 8 GHz VLA (*A*-configuration) map is necessary for this source to be well resolved. All other sources have FR$>$0.7; indicating that the hotspots are close to the leading edge of the lobes. So, all of these quasars radio sources possess FR-II-type morphologies and luminosities, even the eight sources with bending angles $\theta>20°$. The $\theta>20°$ sources resemble the "dogleg" radio structure found by Stocke *et al.* (1985) for 3C 270.1 and 3C 275.1, not the FR-I structure of $z\sim 0$ cluster radio sources.

We use the two-point correlation function amplitude B_{gq} as defined by Longair & Seldner (1979) as a measure of cluster density. Sources with a $B_{\mathrm{gq}}>500$ Mpc$^{-1.8}$ are regarded as being a member of a rich cluster. This criterion is chosen because it is between an Abell (1976) richness class 1 (350 Mpc$^{-1.8}$) and richness class 2 (650 Mpc$^{-1.8}$) cluster (YE93). By this criterion, 8 out of 30 sources (27%) are within a rich cluster. If clusters have had sufficient time to collapse and virialize, stripping the galactic halos and forming a dense ICM at $z\sim\frac{1}{2}$, this should be reflected in the radio galaxy morphology of cluster quasars as compared to non-cluster quasars. But since the cluster density B_{gq} is a measure of galaxy, not ICM, density, a lack of radio galaxy morphology changes with B_{gq} would suggest, but not prove, that at $z\sim\frac{1}{2}$ clusters of galaxies surrounding quasars have not yet formed a dense ICM. It should be noted that the B_{gq} taken from YE93 were calculated from standard cosmology with $H_0=50$ km s^{-1} Mpc^{-1} and $q_0=0$. While this is not consistent with the cosmological model assumed here, this does not significantly affect our measured correlations as the B_{gq} dependence on H_0 roughly scales directly with the Abell richness; and B_{gq} is insensitive to q_0.

The core and total radio powers P^c_{20} and P^t_{20} are calculated from the 20 cm core and total flux values respectively given in the literature assuming isotropic emission. If a 20 cm flux was not available, it was estimated from the 6 cm flux and a power-law spectral index α, where $P_{20}\sim\nu^{\alpha}$.

The following information applies to Table 1: Columns 1 & 2: the IAU designation for the source as well as alternate catalog designations. Column 3: the quasar redshift taken from YE93. Columns 4 & 5: the quasar-galaxy spatial covariance amplitude (in Mpc$^{-1.8}$) and the uncertainty take from YE93. Column 6: radio map references: (A) Antonucci 1985; (G) Gower & Hutchings 1984; (H) Hintzen *et al.* 1983; (M) Morganti *et al.* 1993; (MH) Miley & Hartsuijker 1978; (N) Neff & Brown 1984; (P) Price *et al.* 1993; (PH) Pooley & Henbest 1974; (PW) Potash & Wardle 1979; (S) Stocke (private communication). Column 7: the largest angular size of the source (in arcsec), defined as the separation of the brightest components in the outer lobes. All values were obtained from Nillson *et al.* (1993), except as marked. A dagger indicates the value was obtained from Hintzen *et al.* (1983); an asterisk indicates that the LAS was measured directly from the radio map. Column 8: projected physical size (in kpc). Column 9: the projected bending angle. All values were measured from radio maps. For angles marked with a dagger the bending angle is calculated by using the optical position for the central core. For the angles marked with an asterisk the source is distorted and the bending angle is uncertain (see comments for individual sources). Column 10: the Fanaroff–Riley (1974) ratio measures the hotspot placement in the lobes (see above for a numerical definition). Column 11: the lobe asymmetry Q measures the relative lengths from the core to the hot spots (see above).

The following information applies to Table 2: Column 1: the IAU designation for the source. Columns 2 & 3: the core radio flux (mJy) at 6 and 20 cm, respectively. If a value is not listed, the 20 cm flux is calculated from the 6 cm flux by assuming a power-law spectrum. Column 4: the power-law spectral index of the core. A value of $-\frac{1}{2}$ is assumed for those not listed. Column 5: references for the core flux: (B) Barthel *et al.* 1984; (C) Conway *et al.* 1974; (G) Gower & Hutchings 1984; (H) Hintzen *et al.* 1983; (HR) Hough & Readhead 1989; (Hu) Hutchings *et al.* 1988; (K) Kellermann *et al.* 1989; (PKS) The Parkes survey (Bolten *et al.* 1979). If two references are listed, the second is for the spectral index. Columns 6 & 7: the total radio flux (mJy) at 6 or 20 cm, respectively. If a 20 cm value is not listed, the 20 cm flux is calculated from the 6 cm flux by assuming a spectral index of -0.8. Values marked with an asterisk were estimated from the 2.7 and 5.0 GHz fluxes assuming a power-law spectrum. Column 8: references for the total flux: reference abbreviations are the same as listed for column 5. Columns 9 & 10:

TABLE 3. Linear-correlation coefficients.

	B_{gq}	Size	θ	FR	Q	P_{20}^{c}	P_{20}^{t}
z	0.563	0.032	-0.158	0.206	-0.056	0.314	0.608
B_{gq}		-0.144	0.039	-0.058	-0.163	0.157	0.516
Size			-0.243	0.456	-0.404	-0.050	-0.079
θ				-0.088	-0.130	0.075	-0.202
FR					-0.098	-0.064	0.203
Q						0.028	0.135
P_{20}^{c}							0.090

TABLE 4. Probabilities that distribution arises by chance.

	B_{gq}	Size	θ	FR	Q	P_{20}^{c}	P_{20}^{t}
z	0.002	0.868	0.413	0.283	0.775	0.135	0.001
B_{gq}		0.457	0.840	0.758	0.397	0.463	0.004
Size			0.204	0.013	0.030	0.815	0.677
θ				0.651	0.501	0.730	0.285
FR					0.614	0.765	0.281
Q						0.898	0.478
P_{20}^{c}							0.677

the logarithmic core (where available) and total radio power (W Hz^{-1}) at 20 cm assuming isotropic emission.

4. COMMENTS ON INDIVIDUAL SOURCES

0003+158, 0155−109, 1100+772, 1302−102, 1512+370, and 2209+080: These sources are not fully resolved. The value of the FR ratio is a lower limit because the outer edge of the jets are not resolved and it is probable that the source is more edge brightened than calculated.

0135−057: The central core is not visible; only the outer lobes are detected. The bending angle θ and FR ratio are calculated by using the optical position for the central core. $\theta=65°$ is a lower limit; however it is the most probable value.

0137+012: The object is collinear. However, the northern lobe is considerably larger; possibly suggesting some sort of interaction.

0805+578: The outer lobes are connected by a nearly continuous jet; i.e., the lobes are not clearly separated from the source.

0903+169: 3CR 215 is listed as 0905+167 in YE93; but it is listed in the Hewitt & Burbidge (1987) catalog and other locations as 0903+169. The structure of 0903+169 is very complex and the bending angle is uncertain. It is, however, clearly distorted.

1012+488: θ and FR ratio are calculated by using the optical position for the central core. $5°<\theta<17°$; with $\theta=8°$ the most probable value.

1058+110: It is unclear whether this source is a triple or a double; i.e., whether or not it consists of one or two lobes. There are three components; however, the westernmost component is the brightest. Faint emission to the west also suggests that there is a western lobe not visible in the map. For this reason we have chosen to discard this source.

1103−006: The jets connecting the outer lobes are curved in a way suggesting rotation of the source rather than motion through an external medium. For this reason the bending angle is unclear; it depends upon how the positions of the outer lobes are measured. $1°<\theta<20°$; with $\theta=3°$ the most probable value.

1200−051: The outer lobes are very faint in comparison to the central core. The bending angle is measured with respect to the centers of the outer lobes, which may not be the hot spot locations.

1217+023: The western lobe is not clearly visible; and the bridge to the eastern lobe is sharply bent, suggesting a collision or other catastrophic event. The low surface brightness emission indicates a morphology suggestive of rotation of the source.

1241+166: The curvature of this source (3C 275.1) is suggestive of a collision with a neighboring galaxy because the southern lobe is larger and closer to the central core (Stocke *et al.* 1985). An object on the southern side of 1241+166, which has the same redshift and is collinear with the northern lobe, is the most likely deflector.

1302−102: The low surface brightness gives evidence for jet-like structure which is used to measure the bending angle. However, it is only suggestive of outer lobes so that the FR ratio is merely a lower limit.

1548+114: The outer lobes have multiple bright spots, making the measurement of the bending angle ambiguous. The source is clearly bent between 11° and 58°. Measuring from the brightest components in the lobes, it is most probably bent 47°.

5. RESULTS

The linear-correlation coefficients and chance probabilities for a correlation between each pair of measured variables are listed in Tables 3 and 4. The probabilities indicate the likeliness that the correlation coefficients could have occurred by chance in a random sample of thirty quasars. All lower limits for the FR ratio are treated as points for this analysis. The following correlations are found: redshift z with B_{gq} and core and total power; B_{gq} with total power; and projected physical size with projected bending angle, FR ratio, and length asymmetry. The latter two correlations are included here as a test for consistency within the sample and are not the focus of the paper. They are in general agreement with previous studies of radio-morphological correlations of quasars (e.g., Hough & Readhead 1989, and references therein.)

The B_{gq} and z correlation (Table 3) has been extensively discussed by YE93 and references therein. It is thought to be caused by quasar luminosity evolution; i.e., radio sources in clusters at low redshifts have substantially faded and are called radio galaxies instead of quasars. Since none of the radio morphology parameters correlate with z, the strong dependence of B_{gq} on z does not bias the present study. The

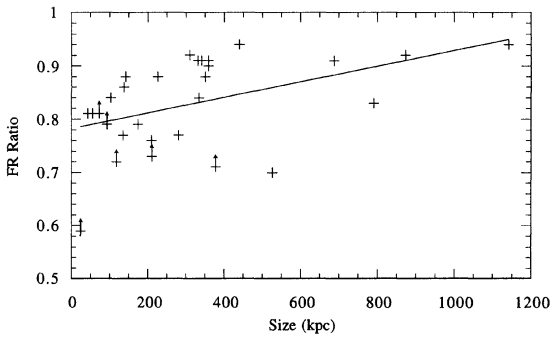

FIG. 2. FR ratio plotted as a function of physical size. Sources marked with an arrow indicate that the FR ratio is a lower limit. The solid line (with slope=1.53×10^{-4} kpc^{-1} and y intercept=0.78) is a good linear fit to the data (correlation coefficient=0.456).

correlation between size and FR ratio is shown in Fig. 2 and is similar to the correlation seen for radio sources at $z\sim0$ (e.g., Stocke 1979) where interaction with a dense ICM is the suspected cause. But this conclusion is also consistent with an inelastic collision between a lobe and a nearby galaxy halo or intergalactic cloud. An inelastic collision would impede expansion of the source; and internal heating of the lobe due to shocks (Stocke *et al.* 1985) would expand the lobe transversely, thus reducing the FR ratio.

The anticorrelation between projected size and bending angle is only at an 80% confidence level (Table 3); and inspection of Fig. 3 suggests that the correlation is not linear. Whether this is more than only a projection effect (Kapahi & Saikia 1982) is unclear. The strong anticorrelation (98% confidence; Table 4) between projected size and length asymmetry is also most likely a projection effect. Light travel time differences between the back and foreground lobes of an intrinsically symmetric source will produce an apparent asymmetry which is dependent on the expansion speed and orientation of the lobes (McCarthy *et al.* 1991). Thus an intrinsically symmetric source oriented with a small angle to the line of sight will appear foreshortened and asymmetric.

We find no correlation between B_{gq} and projected bending angle nor physical size (Figs. 4, 5 and Table 3). This suggests that a dense ICM is not solely responsible for the distorted morphology of these quasars. Some authors (e.g., Barthel

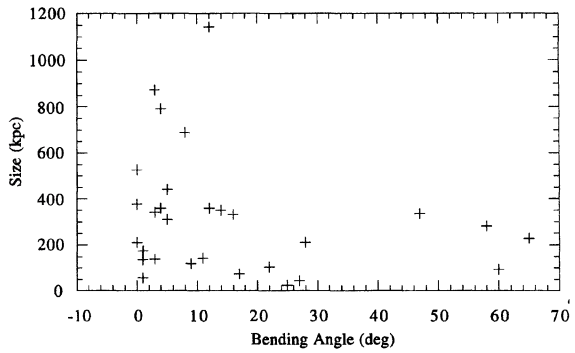

FIG. 3. Projected physical size plotted as a function of projected bending angle θ.

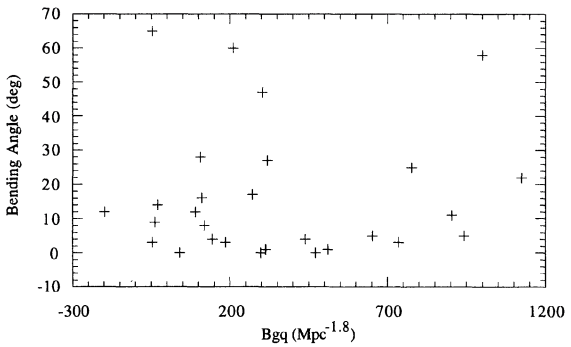

FIG. 4. Projected bending angle plotted as a function of B_{gq}.

1989) have suggested that quasars are FR-II radio galaxies seen at preferred angles, closer to the jet axis. If this is the case, projection effects would cause observed bending angles to be exaggerated. However, few of these sources show large bending angles; thus this effect must not be large in this particular sample of quasars.

The strong correlation between total radio power P^t_{20} and z (Table 4) is a selection effect due to our flux-limited sample. The strong correlation between P^t_{20} and B_{gq} is merely a combination of the P^t_{20} and z correlation and the B_{gq} and z correlation discussed above. However, we do not find any correlation between total or core radio power and the radio morphological parameters. This is inconsistent with the known correlations between radio power and radio morphology (Owen & Ledlow 1994; Fanaroff & Riley 1974) and B_{gq} (Prestage & Peacock 1988; Longair & Seldner 1979) found at $z\sim0$. However, our sample consists only of powerful radio sources within a narrow range of total powers ($24.9<\log P^t_{20}<26.4$) so that all of our sources would be classified as FR-II from their luminosities. Therefore it is not surprising that we do not see the strong radio power/radio morphology correlations found at $z\sim0$. These results do confirm that variations in the core or total radio power do not significantly affect the radio structure; and that another mechanism must be responsible for the large distortions in radio morphology seen in ~14% of these sources.

6. CONCLUSION

It is clear from the radio morphologies and B_{gq} values for this sample that interaction with the ICM is not the sole

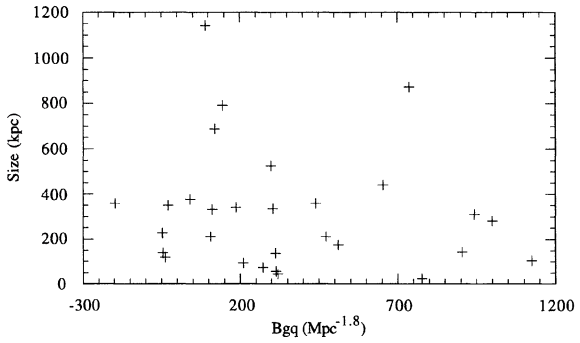

FIG. 5. Projected physical size plotted as a function of B_{gq}.

determinant of the morphology of the quasar. That we see highly bent sources outside of clusters (e.g., 0135−057) indicates that alternative mechanisms for bending sources at $z\sim\frac{1}{2}$ exist; and that it is incorrect to assume that quasars with noncollinear structure are always members of rich clusters, as proposed by Hintzen & Scott (1978). It is also clear that the core radio power for these high-luminosity sources is not a significant factor in determining the differences in radio morphology that are observed. An inelastic collision between one of the lobes and a nearby galaxy halo or intergalactic cloud is a likely explanation for the "dogleg" structure of several of the quasars in our sample as suggested by Stocke *et al.* (1985). These sources do not show the WAT or NAT structure expected of sources moving relative to a dense ICM; nor do they have distorted lobes indicative of interactions with a dense ICM (i.e., FR-I sources). Very few nearby galaxies are necessary to produce the low percentage of highly bent sources (14%, 4 of 29) seen in the sample. In fact, several studies (Guindon 1978; Stocke 1979; Shaver *et al.* 1982) have shown that there are no significantly bent sources which lack close companions. These results also suggest that the distorted morphologies of very high redshift quasars found by Miley & Hartsuijker (1978) may not be due to interaction with a dense ICM either.

This analysis also provides some evidence that rich clusters of galaxies, surrounding quasars at $z\sim\frac{1}{2}$ do not yet possess a dense, hot ICM as is found ubiquitously in rich clusters at $z\sim0$. This conclusion is less secure because all of the quasars used in this study have radio power levels consistent with a FR-II classification. Although we find no evidence for correlations between radio power and any radio morphological parameters, radio power levels similar to those found for nearby cluster radio galaxies are not present in the sample investigated herein. Deep radio and optical imaging as well as sensitive ($f_x<10-13$ ergs s^{-1} cm^{-2}), high-resolution (<5 arcsec) soft x-ray imaging of a sample of lower power radio galaxies at $z\sim\frac{1}{2}$ will be required to adequately test this hypothesis.

J.T.S. acknowledges support by NSF Grant No. AST-9020008 and NASA LTSA Grant No. NAGW-2645 for this work. T.A.R. acknowledges support from a NASA Graduate Student Research Grant No. NGT-50909. E.E. acknowledges support from NASA/HST archival Grant No. AR-4682.01-92A.

REFERENCES

Abell, G. O. 1976, in Galaxies and the Universe, edited by A. Sandage, M. Sandage, and M. Kristian (University of Chicago Press, Chicago), Vol. 9
Antonucci, R. R. J. 1985, ApJS, 59, 499
Barthel, P. D., Miley, G. K., Schilizzi, R. T., & Preuss, E. 1984, A&A, 140, 821
Barthel, P. D. 1989, ApJ, 336, 606
Bolten, *et al.* 1979, Australian J. Phys., Astrophys. Supp., No. 46 (and references therein)
Conway, R. G., Haves, P., Kronberg, P. P., Stannard, D., Vallée, J. P., & Wardle, J. F. C. 1974, MNRAS, 168, 137
De Young, D. S. 1976, ARA&A, 14, 447
Ellingson, E., Yee, H. K. C., & Green, R. F. 1991, ApJ, 371, 36
Fanaroff, B. L., & Riley, J. M. 1974, MNRAS, 167, 31P
Forman, W., & Jones, C. 1982, ARA&A, 20, 547
Gower, A. C., & Hutchings, J. B. 1984, AJ, 89, 1658
Guindon, B. 1978, MNRAS, 183, 195
Hewitt, A., & Burbidge, G. 1987, ApJS, 63, 1
Hintzen, P., & Scott, J. 1978, ApJ, 224, L47
Hintzen, P., Ulvestad, J., & Owen, F. N. 1983, AJ, 88, 709
Hough, D. H., & Readhead, A. C. S. 1989 AJ, 98, 1208
Hutchings, J. B., Price, R., & Gower, A. C. 1988, ApJ, 329, 122
Jaffe, W., & Perola, C. 1973, A&A, 26, 423
Jones, T., & Owen, F. N. 1979, ApJ, 234, 818
Kapahi, V., & Saikia, D. 1982, A&A, 3, 161
Kellermann, K. I., Sramek, R., Schmidt, M., Shaffer, D. B., & Green, R. 1989, AJ, 98, 1195
Longair, M., & Seldner, M. 1979, MNRAS, 189, 433
McCarthy, P. J., van Breugel, W., & Kapahi, V. K. 1991, ApJ, 371, 478
Miley, G., & Hartsuijker, A. 1978, A&AS, 34, 129
Morganti, R. Killeen, N. E. B., & Tadhunter, C. N. 1993, MNRAS, 263, 1023
Neff, S. G., & Brown, R. L. 1984, AJ, 89, 195
Nillson, K., Valtonen, M. J., Kotilainen, J., & Jaakkola, T. 1993, ApJ, 413, 453
Owen, F. N., & Ledlow, M. J. 1994, ASP Conf. Ser. 54, edited by G. V. Bicknell, M. A. Dopita, and P. J. Quinn (BookCrafters, Inc., San Francisco)
Pooley, G., & Henbest, S. 1974, MNRAS, 169, 477
Potash, R. I., & Wardle, J. F. C. 1979, AJ, 84, 707
Prestage, R. M., & Peacock, J. A. 1988. MNRAS, 230, 131
Price, R., Gower, A. C., Hutchings, J. B., Talon, S., Duncan, D., & Ross, G. 1993, ApJS, 86, 365
Shaver, P. *et al.* 1982, in Extragalactic Radio Sources, IAU Symposium No. 97, edited by D. S. Heeschen and C. M. Wade (Reidel, Dordrecht), p. 55
Stocke, J. T. 1979, ApJ, 230, 40
Stocke, J. T., Burns, J. O., & Christiansen, W. A. 1985, ApJ, 299, 799
Yee, H. K. C., & Ellingson, E. 1993, ApJ, 411, 43 (YE93)